Nanospheres

DOI: 10.1002/ange.201105486

Synthesis of Discrete and Dispersible Hollow Carbon Nanospheres with High Uniformity by Using Confined Nanospace Pyrolysis**

An-Hui Lu, Tao Sun, Wen-Cui Li, Qiang Sun, Fei Han, Dong-Hai Liu, and Yue Guo*

In recent years, hollow carbon nanospheres (HCSs) have attracted a great deal of attention because of their unique properties such as high surface-to-volume ratios, and excellent chemical and thermal stabilities.[1] In this regard, HCSs are superior to polymer- and metal-based hollow nanospheres.[2,3] HCSs are promising materials in a variety of applications such as adsorption,[4] lithium ion batteries,[5] fuel cells,[6] and catalysis,[7] and can also serve as building blocks for complex structures.[2] The success of HCSs in these applications relies strongly on the availability of HCSs with carefully controlled diameter and shell thickness, surface properties, crystallinity of the carbon shell, and dispersibility in media. Much effort has been devoted to the synthesis of HCSs by a nanocasting approach.[8] However, most previous reports on HCSs have the sole aim of obtaining hollow structural units, and little attention has been paid to addressing the issue of particle conglutination. In fact, an inevitable tendency of all carbon nanostructures during high-temperature annealing is the incidental condensing and sintering. Consequently, the end results are often nondispersible and conglutinated bulky materials. This challenge becomes even greater when the carbon particles are smaller, for example, below 200 nm.[9] Discrete and dispersible HCSs are of critical importance for both the fundamental study of carbon colloids and for many practical applications such as colloidal catalysts, drug carriers, nanodevices, and inks. However, to the best of our knowledge, no feasible solution has been reported to date that can satisfactorily resolve the issue of conglutination for carbon nanoparticles. Thus, it remains a great challenge to develop a simple and effective strategy to overcome the barrier and to produce discrete and dispersible HCSs with high uniformity.

Herein, we describe a new method referred to as "confined nanospace pyrolysis" for the synthesis of discrete and highly dispersible HCSs that have both tailorable shell thickness and cavity size. This idea is inspired from nature, in particular the structure of an egg, which consists of an inorganic outer shell (eggshell), organic inner shell (egg white), and core (yolk). The presence of the inorganic outer shell is an essential element that ensures that eggs retain their original shape, and remain discrete. A designed synthesis of HCSs that was inspired by the egg structure is illustrated in Figure 1a. Firstly, monodisperse polystyrene nanospheres (PS) with a specific particle size are prepared as the seed;

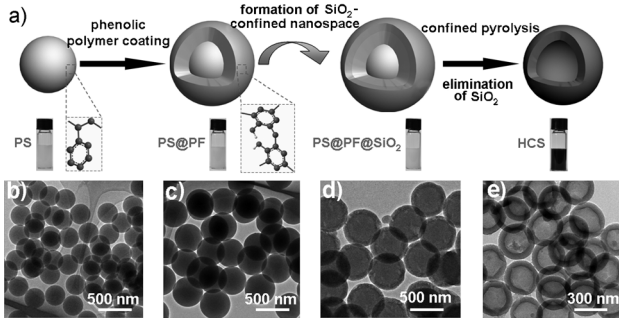

Figure 1. a) Confined nanospace pyrolysis of hollow carbon nanospheres, insets show photographs of the stable aqueous suspensions of the products. TEM images of the product obtained from each step: b) PS, c) PS@PF, d) PS@PF@SiO_2, and e) HCS.

secondly, the surface of the PS seed is uniformly coated with a highly cross-linked polymer that is produced from the precursors phenol and formaldehyde (PF) by a hydrothermal method and forms the inner shell; the as-synthesized product is denoted PS@PF. The third step, which is crucial for obtaining discrete and dispersible HCS, involves the formation of an inorganic outer silica shell that functions as a nanoreactor to provide a confined nanospace for the high-temperature pyrolysis of the PF polymer and also as a boundary to prevent polymer/carbon conglutination during high-temperature treatment. This product with a single core and dual-shell structure is denoted PS@PF@SiO_2. In this way, each single PF polymer nanosphere can be converted to carbon within only the isolated nanoreactor of the inorganic silica shell during pyrolysis. Meanwhile, the PS seed decomposes to leave a void in the carbon product. Finally, discrete and dispersible HCSs are obtained after pyrolysis of the PS@PF@SiO_2 and subsequent elimination of the nanoreactor silica. The products from each step were monitored by using TEM.

As seen from Figure 1b, the PS seed was prepared with a uniform size of (250 ± 2) nm by a modification of a reported method.[10] To ensure a uniform coating of PF on PS, the dispersity of PS in aqueous solution is crucial. Thus, the zeta potential of PS was measured in aqueous solution as a function of pH value. As shown in Figure 2a, the surface of

[*] Prof. A.-H. Lu, T. Sun, Prof. W.-C. Li, Q. Sun, F. Han, D.-H. Liu, Y. Guo
State Key Laboratory of Fine Chemicals
School of Chemical Engineering
Dalian University of Technology, Dalian 116024 (P.R. China)
E-mail: anhuilu@dlut.edu.cn

[**] The project was supported by the NSFC (nos. 20873014 and 21073026), the Program for New Century Excellent Talents in University of China (NCET-09-0254), and the Scientific Research Foundation for the Returned Overseas Chinese Scholars.

Supporting information for this article is available on the WWW under http://dx.doi.org/10.1002/anie.201105486.

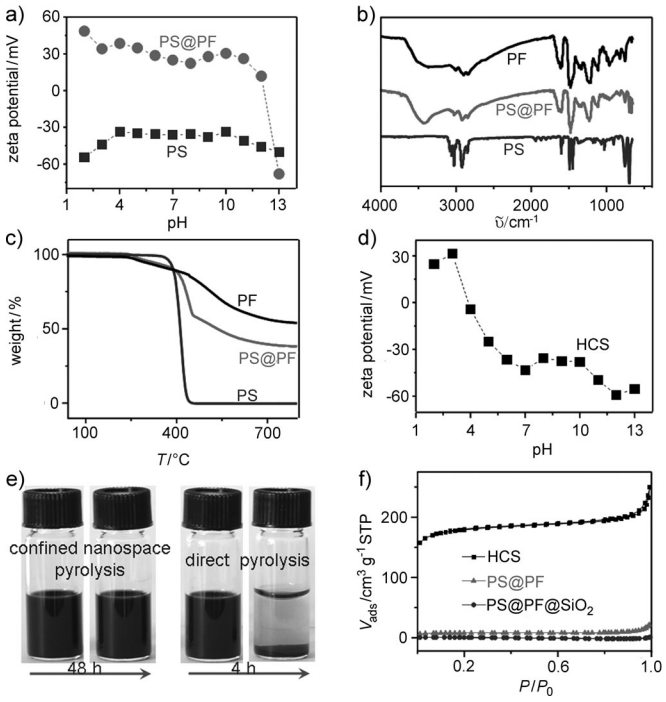

Figure 2. Zeta potentials of the obtained a) PS, PS@PF and d) HCS in aqueous solution at different pH values; b) FTIR spectra and c) TG curves of PF, PS@PF, and PS; e) photographs of the dispersed solution of HCSs obtained from PS@PF with and without confined nanospace pyrolysis; and f) nitrogen sorption isotherms of HCS, PS@PF, and PS@PF@SiO_2.

the PS is negatively charged. Over the total pH range, the absolute values of the zeta potentials are all above 30, which indicates that PS can be stably dispersed in aqueous solution, thus allowing an easy manipulation of the surface coating of PS with PF. The pH values of the solution used for PF coating before and after hydrothermal synthesis are approximately 7 and 10, respectively. The π–π interaction between PS and phenol molecules possibly enables the formation of the phenol-containing polymer on the surface of the PS nanosphere by formation of a PS@PF core–shell structure. Figure 1c shows the TEM image of the intermediate product PS@PF sampled in the second step. The diameter of PS@PF increased from (250 ± 2) to (360 ± 3) nm, thus suggesting a successful coating of PF around the surface of the PS spheres. The thickness of the coated PF layer was estimated to be approximately 55 nm. However, a core–shell structure could not be observed in the TEM image of the PS@PF spheres because of the similar electron contrast between PS and PF. To create a confined pyrolysis nanospace, PS@PF nanospheres were coated with a silica shell by the modified Stöber method.[11] The zeta potential measurements of PS@PF indicate that their surfaces are positively charged and they can form a stable suspension when the pH value is 10 or lower. We therefore adjusted the pH of the silica coating system to approximately 10. As a result, a typical core–shell structure 440 nm in diameter and with a silica shell thickness of around 40 nm was obtained, thus indicating a successful coating of PS@PF with silica (Figure 1d). The electrostatic interaction between the positively charged PS@PF surface and the hydrolyzed negatively charged silica moieties is considered to be the driving force that results in the successful surface coating with silica.[12] After pyrolysis of the polymer and subsequent elimination of the confined nanoreactor, discrete and uniform HCSs (ca. 300 nm) are produced (Figure 1e). The resulting HCSs are dispersible in an aqueous solution, and have a hollow core 220 nm in diameter and shell with a thickness of 40 nm. The size of the hollow core is smaller than that of the PS seed (ca. 250 nm), and is believed to be the result of PF contraction at higher temperatures. The formation of a hollow core indicates that the carbon shell is porous and thus allows the escape of the decomposed PS moieties.

To further confirm the surface coating of PS with PF, the samples PF, PS, and PS@PF were characterized by using FTIR spectroscopy. As seen in Figure 2b, the spectra of PF and PS@PF show a broad band at 3500 cm^{-1}, which arises from the vibrational stretching of the OH groups. The weak bands at 2860–2969 cm^{-1} are related to the alkyl C–H stretching in the CH_2 unit. The strong band at 1580–1600 cm^{-1} is attributed to an aromatic ring stretching vibration. The band at 1240 cm^{-1} can be assigned to the C–O vibrational stretching, which is also the prominent characteristic absorption of PF that is not observed for PS. In addition, the characteristic peaks of PS (3060, 3030, 2920, 2850, 1600, 1490, 1450, 756, 700 cm^{-1}) can also be found in the spectrum of PS@PF nanospheres, in particular, the peak at 700 cm^{-1} that arises from the out-of-plane deformation mode of C–H in single substituted benzene rings. Thus, the IR results indicate that the PS surface was coated with the PF polymer.

The thermal behavior of the samples of PS, PF, and PS@PF were also investigated by using thermogravimetry (TG; Figure 2c). In the case of PS, weight loss began at 350 °C and 100 % weight loss was reached before 450 °C, thus indicating that the PS seeds used in this study can be completely removed by pyrolysis at high temperature. This observation is consistent with previous studies.[9b] In contrast, PF shows a carbon conversion of approximately 54 % at 800 °C. The TG curve of PS@PF exhibits a weight loss beginning at 250 °C. Weight losses of 6.5 % and 32.2 % are observed in the temperature ranges of 250–350 °C and 350–450 °C, respectively. These losses are attributed to water removal from the condensation of PF and the predominant decomposition of PS, respectively. Finally, PS@PF gives a carbon yield of 38 % at 800 °C. Based on the spherical sizes determined by TEM observations and the approximate densities of PS and PF of 1 $g cm^{-3}$[13] and 1.2 $g cm^{-3}$,[14] respectively, a mass ratio between PS and PF of 29.6:70.4 can be estimated. When the carbon yield of 54 % from pure PF at 800 °C is taken into account, the yield of PS@PF would be 38.0 % (see the Supporting Information for details). This result is in good agreement with the TG data.

Zeta potentials of the obtained HCSs were measured in aqueous solution at different pH values. As shown in Figure 2d, the surface charge of the HCSs switched from positive to negative with an increase in pH values from 2 to 13. In the pH range of 5–13, the absolute zeta potential value of the HCSs is above 30, which indicates that these species can be

stably dispersed in aqueous solution. As shown in Figure 2e, the dispersed solution of the HCSs is very stable, with no sign of aggregated precipitation over 2 days. Only after 5 days did the very upper part of the solution start to become slightly less dark than the lower part, however, no sediment was observed. Noticeably, since we did not use any surfactant or polymer for facilitating the stabilization of the HCSs, such a stable dispersion results mainly from electrostatic repulsion. In contrast, when PS@PF is directly subjected to pyrolysis (see the TEM image in Figure S1), the resultant HCSs are not dispersible in water, as evidenced by the visible sediment at the bottom of the sample vial. This behavior is even more evident when the pyrolysis temperature is higher, for example, 800 °C. Thus, we are not able to measure the zeta potentials of these directly pyrolyzed particles because they form sediments in aqueous solutions at different pH values. This behavior is a strong indication that the confined nanospace pyrolysis technique ensures the formation of discrete and dispersible HCSs. To the best of our knowledge, this is the first report of the preparation of discrete, highly uniform carbon-based colloidal hollow nanospheres.

Nitrogen adsorption at −196 °C was used to measure the porosity of the obtained samples. As shown in Figure 2f, the N_2 sorption isotherms clearly demonstrate the microporosity of these HCSs as they have a high nitrogen uptake, while the samples PS@PF and PS@PF@SiO_2 have very low porosity. The PS@PF nanospheres have a very small surface area (10.6 $m^2 g^{-1}$), as does PS@PF@SiO_2 (1.9 $m^2 g^{-1}$). In contrast, a dramatic increase in the surface area of the final HCS product (603.8 $m^2 g^{-1}$) is observed and is accompanied by a large increase in pore volume (0.32 $cm^3 g^{-1}$ at $P/P_0 = 0.95$).

The above results have shown that confined nanospace pyrolysis is a practical technique for the production of discrete, dispersible, and uniform HCSs. We further demonstrated that the diameter, hollow core size, and shell thickness are also tailorable by tuning the synthesis conditions. The SEM images in Figure 3a–d show that HCSs with diameters of (440 ± 4), (330 ± 4), (290 ± 4) and (100 ± 10) nm can be synthesized. These HCSs are derived from the PS seeds with sizes of (360 ± 2), (280 ± 2), (200 ± 2), and (40 ± 8) nm (inset images in Figure 3a–d). TEM was used to determine the hollow core sizes and the shell thicknesses of these HCSs. As shown in Figure 3e–h, the hollow core sizes of the HCSs are (310 ± 2), (245 ± 2), (180 ± 2), and (38 ± 8) nm, and the shell thicknesses are (35 ± 2), (45 ± 2), (70 ± 2), and (30 ± 2) nm, respectively. In addition, the shell thickness is also tuneable by simply altering the molar ratio of the PF precursor to the PS template. For example, when using 200 nm PS spheres as the seeds, two different HCSs (Figure 3i,j) can be prepared with the same core diameter of 180 nm, but with a shell thickness of either 30 or 80 nm. As expected, these products are dispersible in water to form stable suspensions. For example, the representative DLS curves of two different HCSs (HCS-440 and HCS-330; the number represents the diameter of a HCS in nm) show that the determined particle sizes are very close to those measured by SEM and TEM. More importantly, the polydispersity index of these HCSs is approximately 5% (Figure 3k), thus indicating a high uniformity in the sizes of these products.[15a] Hence, the versatility

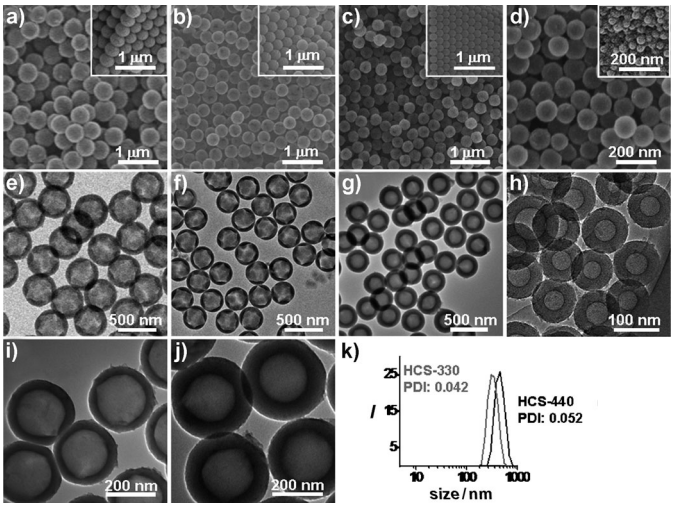

Figure 3. Characterization results of the series of HCSs with tunable sizes. SEM images of HCSs with diameters of a) (440 ± 4), b) (330 ± 4) nm, c) (290 ± 4), and d) (100 ± 10) nm; the insets show images of the PS nanospheres: a) (360 ± 2), b) (280 ± 2), c) (200 ± 2), and d) (38 ± 8) nm. The corresponding TEM images of these HCSs are shown in (e–h), their core sizes are e) (310 ± 2), f) (245 ± 2), g) (180 ± 2), and h) (40 ± 8) nm. TEM images (i and j) show HCSs with identical core size of ca. 180 nm but varied shell thickness: i) 30 nm and j) 80 nm. k) Representative DLS curves of the HCSs (HCS-440 and HCS-330). PDI = polydispersity index.

of our synthesis towards discrete, dispersible, and uniform HCSs has been successfully demonstrated.

To demonstrate an application of these structures, the HCSs can be activated further to increase the surface area and subsequently used as an effective adsorbent for the fast removal of organic waste in aqueous solution. As an example, the time-resolved adsorption capacities of phenol on different adsorbents are shown in Figure S2. Remarkably, steam activation led to a significant increase in the specific surface area and porosity (Figure S3 and Table S1) of the sample HCS-240. Thus, the adsorption of phenol for sample of activated HCS-240 is higher (ca. 251 $mg g^{-1}$) than that of HCS-240 (ca. 137 $mg g^{-1}$) and commercial PICA activated carbon (ca. 224 $mg g^{-1}$). Noticeably, within one minute, both the original and the activated HCSs show higher adsorption rates than that of commercial activated carbon. The faster adsorption rate (kinetics) is attributed to the developed and directly accessible porosity of these nanosized hollow spheres.

In summary, we have demonstrated a new concept, namely confined nanospace pyrolysis, to produce individual, dispersible, and uniform HCSs by consecutive surface coating on spherical PS seeds. More importantly, our approach ensures that even after pyrolysis at a high temperature, the particle coagulation that was commonly encountered for carbonaceous materials can be eliminated. This technique allows the preparation of HCSs in a dispersible state, which is particularly important in the application fields where strict control of the monodispersity, particle sizes, and dispersibility of the HCSs is necessary. The HCSs obtained by using this method show not only great promise for many applications such as advanced storage materials, adsorbents, catalyst

supports, drug delivery carriers, and templates, but also an ideal model system for exploring the physical and chemical properties of carbon colloids. It is easy to envisage that this confined nanospace pyrolysis strategy can also been applied to the preparation of solid carbon nanospheres[15b] in a dispersible state.

Experimental Section

Typical synthesis of 360 nm PS spheres: Styrene (3.5 mL, 30 mmol) and oleic acid (94 μL) were dissolved in water (141 mL), and the solution was stirred at 50 °C for 1 h. Potassium persulfate (78 mg, 0.288 mmol) was added and the solution was heated to 70 °C under vigorous stirring for 5 h. All steps were performed under argon. The PS spheres were separated by centrifugation and washed three times with water. The syntheses of 40, 200, and 280 nm PS spheres are described in the supporting information.

Typical synthesis of PS@PF nanospheres: 360 nm PS spheres (150 mg) were dispersed in water (100 mL), then an aqueous solution (20 mL) of phenol (0.188 g, 2.0 mmol) and hexamethylenetetramine (0.14 g, 1 mmol) was added. After stirring gently for about 5 min, the solution was transferred into a 150 mL Teflon-lined autoclave and heated at 160 °C for 4 h. The PS@PF spheres were collected by centrifugation and washed several times with water and pure ethanol.

Synthesis of PS@PF@SiO_2 nanospheres: Cetyltrimethylammonium bromide (0.48 g, 1.32 mmol) was stirred with water (15 mL) for 1 h at 30 °C. This solution was added to a mixture of PS@PF (120 mg), pure ethanol (30 mL), water (75 mL), and ammonia solution (28 %; 1.2 mL). The solution was stirred for 30 min and then tetraethyl orthosilicate (0.84 mL 3.76 mmol) was added. The reaction mixture was kept at 30 °C for 16 h. PS@PF@SiO_2 was isolated by centrifugation and dried at 50 °C for 10 h.

Synthesis of hollow carbon nanospheres: The as-prepared PS@PF@SiO_2 was heated at 5 °C min^{-1} from room temperature to 150 °C and kept at this temperature for 1 h under a nitrogen flow. The temperature was then raised at 5 °C min^{-1} to 600 °C (or 800 °C), and kept at this temperature for 2 h. The pyrolyzed product was treated with aqueous NaOH solution (2.5 M) to remove the silica and generate HCSs.

Received: August 3, 2011
Revised: September 16, 2011
Published online: October 13, 2011

Keywords: carbon · cross-linking · pyrolysis · nanostructures · silica

[1] a) X. M. Sun, Y. D. Li, *Angew. Chem.* **2004**, *116*, 607 – 611; *Angew. Chem. Int. Ed.* **2004**, *43*, 597 – 601; b) A.-H. Lu, W. C. Li, G. P. Hao, B. Spliethoff, H. J. Bongard, B. B. Schaack, F. Schüth, *Angew. Chem.* **2010**, *122*, 1659 – 1662; *Angew. Chem. Int. Ed.* **2010**, *49*, 1615 – 1618; c) Z. B. Lei, Z. W. Chen, X. S. Zhao, *J. Phys. Chem. C* **2010**, *114*, 19867 – 19874; d) R. J. White, K. Tauer, M. Antonietti, M. M. Titirici, *J. Am. Chem. Soc.* **2010**, *132*, 17360 – 17363; e) L. M. Guo, J. M. Zhang, Q. J. He, L. X. Zhang, J. J. Zhao, Z. Y. Zhu, W. Wu, J. Zhang, J. L. Shi, *Chem. Commun.* **2010**, *46*, 7127 – 7129.

[2] a) U. Jeone, Y. Wang, M. Ibisate, Y. Xia, *Adv. Funct. Mate*r. **2005**, *15*, 1907 – 1922; b) J. Zhang, Y. Li, X. Zhang, B. Yang, *Adv. Mater.* **2010**, *22*, 4249 – 4269.

[3] a) Y. N. Xia, B. Gates, Y. D. Yin, Y. Lu, *Adv. Mater.* **2000**, *12*, 693 – 703; b) R. P. A. Dullens, *Soft Mater.* **2006**, *2*, 805 – 810; c) H. X. Zhang, H. Zhao, J. X. Wang, J. F. Chen, Y. F. Lu, J. Yun, *Small* **2009**, *5*, 1846 – 1849; d) R. Hao, R. J. Xing, Z. C. Xu, Y. L. Hou, S. Gao, S. H. Sun, *Adv. Mater.* **2010**, *22*, 2729 – 2742; e) R. Costi, A. E. Saunders, U. Banin, *Angew. Chem.* **2010**, *122*, 4996 – 5016; *Angew. Chem. Int. Ed.* **2010**, *49*, 4878 – 4897; f) F. Li, D. P. Josephson, A. Stein, *Angew. Chem.* **2011**, *123*, 378 – 409; *Angew. Chem. Int. Ed.* **2011**, *50*, 360 – 388; g) C. J. Jia, F. Schüth, *Phys. Chem. Chem. Phys.* **2011**, *13*, 2457 – 2487.

[4] a) L. Guo, L. Zhang, J. Zhang, J. Zhou, Q. He, S. Zeng, X. Cui, J. Shi, *Chem. Commun.* **2009**, 6071 – 6073; b) Y. Zhang, S. Xu, Y. Luo, S. Pan, H. Ding, G. Li, *J. Mater. Chem.* **2011**, *21*, 3664 – 3671.

[5] a) N. Jayaprakash, J. Shen, S. S. Moganty, A. Corona, L. A. Archer, *Angew. Chem.* **2011**, *123*, 6026 – 6030; *Angew. Chem. Int. Ed.* **2011**, *50*, 5904 – 5908; b) S. B. Yang, X. L. Feng, L. J. Zhi, Q. Cao, J. Maier, K. Müllen, *Adv. Mater.* **2010**, *22*, 838 – 842; c) W.-M. Zhang, J.-S. Hu, Y.-G. Guo, S.-F. Zheng, L.-S. Zhong, W.-G. Song, L.-J. Wan, *Adv. Mater.* **2008**, *20*, 1160 – 1165; d) Y. Wang, F. Su, J. Y. Lee, X. S. Zhao, *Chem. Mater.* **2006**, *18*, 1347 – 1353.

[6] a) J. H. Kim, J.-S. Yu, *Phys. Chem. Chem. Phys.* **2010**, *12*, 15301 – 15308; b) B. Fang, J. H. Kim, C. Lee, J.-S. Yu, *J. Phys. Chem. C* **2008**, *112*, 639 – 645.

[7] a) Z. L. Schaefer, M. L. Gross, M. A. Hickner, R. E. Schaak, *Angew. Chem.* **2010**, *122*, 7199 – 7202; *Angew. Chem. Int. Ed.* **2010**, *49*, 7045 – 7048; b) Y. Zeng, X. Wang, H. Wang, Y. Dong, Y. Ma, J. Yao, *Chem. Commun.* **2010**, *46*, 4312 – 4314; c) T. Harada, S. Ikeda, Y. H. Ng, T. Sakata, H. Mori, T. Torimoto, M. Matsumura, *Adv. Funct. Mater.* **2008**, *18*, 2190 – 2196; d) R. Liu, S. M. Mahurin, C. Li, R. R. Unocic, J. C. Idrobo, H. Gao, S. J. Pennycook, S. Dai, *Angew. Chem.* **2011**, *123*, 6931 – 6934; *Angew. Chem. Int. Ed.* **2011**, *50*, 6799 – 6802.

[8] a) S. B. Yoon, K. Sohn, J. Y. Kim, C. H. Shin, J. S. Yu, T. Hyeon, *Adv. Mater.* **2002**, *14*, 19 – 21; b) X. W. Lou, D. Deng, J. Y. Lee, L. A. Archer, *Chem. Mater.* **2008**, *20*, 6562 – 6566; c) Y. Xia, R. Mokaya, *Adv. Mater.* **2004**, *16*, 886 – 891.

[9] a) G. G. Qi, Y. B. Wang, L. Estevez, A. K. Switzer, X. N. Duan, X. F. Yang, E. P. Giannelis, *Chem. Mater.* **2010**, *22*, 2693 – 2695; b) J. W. Fu, Q. Xu, J. F. Chen, Z. M. Chen, X. B. Huang, X. Z. Tang, *Chem. Commun.* **2010**, *46*, 6563 – 6565.

[10] A. J. Paine, W. Luymes, J. McNulty, *Macromolecules* **1990**, *23*, 3104 – 3109.

[11] W. Stöber, A. Fink, E. Bohn, *J. Colloid Interface Sci.* **1968**, *26*, 62 – 69.

[12] K. J. C. van Bommel, S. Shinkai, *Langmuir* **2002**, *18*, 4544 – 4548.

[13] N. Tagawa, A. Masuhara, T. Onodera, H. Kasai, H. Oikawa, *J. Mater. Chem.* **2011**, *21*, 7892 – 7894.

[14] D. Jiang, A. C. T. Duin, W. A. Goddard III, S. Dai, *J. Phys. Chem. A* **2009**, *113*, 6891 – 6894.

[15] a) P. Jiang, J. F. Bertone, V. L. Colvin, *Science* **2001**, *291*, 453 – 457; b) J. Liu, S. Z. Qiao, H. Liu, J. Chen, A. Orpe, D. Zhao, G. Q. Lu, *Angew. Chem.* **2011**, *123*, 6069 – 6073; *Angew. Chem. Int. Ed.* **2011**, *50*, 5947 – 5951.

